JOURNAL OF VIROLOGY, June 2008, p. 5940–5950 Vol. 82, No. 12
0022-538X/08/$08.00+0 doi:10.1128/JVI.02496-07

Sulfatide Is Required for Efficient Replication of Influenza A Virus▽

Tadanobu Takahashi,[1,2] Kouki Murakami,[1,2] Momoe Nagakura,[1,2] Hideyuki Kishita,[1,2] Shinya Watanabe,[1,2] Koichi Honke,[2,3] Kiyoshi Ogura,[4] Tadashi Tai,[4] Kazunori Kawasaki,[5] Daisei Miyamoto,[1,2] Kazuya I. P. J. Hidari,[1,2] Chao-Tan Guo,[2,6] Yasuo Suzuki,[2,6] and Takashi Suzuki[1,2]*

Department of Biochemistry, University of Shizuoka, School of Pharmaceutical Sciences and Global COE Program for Innovation in Human Health Sciences, Shizuoka 422-8526, Japan[1]; CREST, Japan Science and Technology Agency, Saitama 332-0012, Japan[2]; Department of Molecular Genetics, Kochi University Medical School, Nankoku, Kochi 783-8505, Japan[3]; Department of Tumor Immunology, Tokyo Metropolitan Institute of Medical Science, The Tokyo Metropolitan Organization for Medical Research, 3-18-22, Honkomagome, Bunkyo-Ku, Tokyo 113-8613, Japan[4]; Institute for Biological Resources and Functions, National Institute of Advanced Industrial Science and Technology (AIST), Tsukuba 305-8566, Japan[5]; and Department of Biomedical Sciences, College of Life and Health Sciences, Chubu University, 1200 Matsumoto-cho, Kasugai-shi, Aichi 487-8501, Japan[6]

Received 21 November 2007/Accepted 5 April 2008

Sulfatide is abundantly expressed in various mammalian organs, including the intestines and trachea, in which influenza A viruses (IAVs) replicate. However, the function of sulfatide in IAV infection remains unknown. Sulfatide is synthesized by two transferases, ceramide galactosyltransferase (CGT) and cerebroside sulfotransferase (CST), and is degraded by arylsulfatase A (ASA). In this study, we demonstrated that sulfatide enhanced IAV replication through efficient translocation of the newly synthesized IAV nucleoprotein (NP) from the nucleus to the cytoplasm, by using genetically produced cells in which sulfatide expression was down-regulated by RNA interference against *CST* mRNA or overexpression of the *ASA* gene and in which sulfatide expression was up-regulated by overexpression of both the *CST* and *CGT* genes. Treatment of IAV-infected cells with an antisulfatide monoclonal antibody (MAb) or an anti-hemagglutinin (HA) MAb, which blocks the binding of IAV and sulfatide, resulted in a significant reduction in IAV replication and accumulation of the viral NP in the nucleus. Furthermore, antisulfatide MAb protected mice against lethal challenge with pathogenic influenza A/WSN/33 (H1N1) virus. These results indicate that association of sulfatide with HA delivered to the cell surface induces translocation of the newly synthesized IAV ribonucleoprotein complexes from the nucleus to the cytoplasm. Our findings provide new insights into IAV replication and suggest new therapeutic strategies.

Influenza A virus (IAV) hemagglutinin (HA) and neuraminidase (NA) are known to associate with specific membrane microdomains (lipid rafts) for assembly and budding of progeny virus (31, 44). Lipid rafts, which are comprised of densely packed cholesterol and sphingolipids, have been shown to be involved in the regulation of various cellular events, including membrane transport (32), virus entry/budding (2), and signal transduction (34). Sulfatide is one of the major sulfated glycolipids abundantly detected in lipid rafts of plasma membranes (3, 26), various mammalian organs (6, 8, 10), and cell lines of mammalian kidneys, which are used for the primary isolation and cultivation of IAVs (23, 24). Sulfatide interacts with extracellular matrix proteins (40), adhesion molecules (1, 14), growth factor (14), bacteria (12), and viruses (7, 36).

The biosynthesis of sulfatide is carried out by the transferases ceramide galactosyltransferase (CGT) and cerebroside (galactosylceramide) sulfotransferase (CST) in the Golgi apparatus (10, 13). CGT converts ceramide to galactosylceramide, a sulfatide precursor. The synthesis of sulfatide follows 3′-O sulfation of galactosylceramide by CST, while specific degradation of sulfatide is performed in lysosomes by arylsulfatase A (ASA), which catalyzes desulfation of galactose residues within sulfatide molecules (Fig. 1) (35).

We previously found that sulfatide binds to IAV particles and inhibits viral infection and sialidase activity under low-pH conditions (36, 38); however, the role of sulfatide in IAV infection remains unknown. In the present study, we investigated the function of sulfatide in the virus infection cycle by knockdown of sulfatide expression in Madin-Darby canine kidney (MDCK) cells, which are known to adequately support IAV replication, and by genetic up-regulation of sulfatide expression in COS-7 cells, which lack sulfatide expression and sufficient IAV replication. We found by using genetically produced sulfatide knockdown or sulfatide-enriched cells that sulfatide regulates translocation of the newly synthesized viral nucleoprotein (NP) from the nucleus to the cytoplasm. Treatment of IAV-infected cells with an antisulfatide monoclonal antibody (MAb) or an anti-HA MAb, which blocks the binding of IAV and sulfatide, resulted in a significant reduction in IAV replication and accumulation of the viral NP in the nucleus. Furthermore, antisulfatide MAb protected mice against a lethal challenge with pathogenic influenza A/WSN/33 (H1N1)

* Corresponding author. Mailing address: Department of Biochemistry, University of Shizuoka, School of Pharmaceutical Sciences, Shizuoka 422-8526, Japan. Phone: 81-054-264-5725. Fax: 81-054-264-5723. E-mail: Suzukit@u-shizuoka-ken.ac.jp.
▽ Published ahead of print on 16 April 2008.

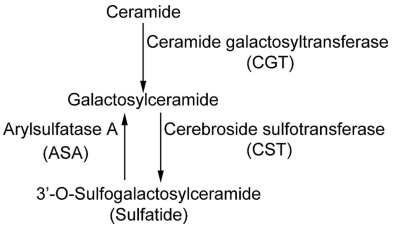

FIG. 1. Metabolism of sulfatide synthesis and degradation.

virus. These results indicate that association of sulfatide with HA delivered to the cell surface induces translocation of the newly synthesized IAV ribonucleoprotein complexes from the nucleus to the cytoplasm, resulting in a remarkable enhancement of IAV replication.

MATERIALS AND METHODS

Cells and viruses. Parent MDCK cells and plasmid-transfected MDCK cells were maintained in Eagle's minimum essential medium supplemented with 5% fetal bovine serum (FBS). COS-7 cells and plasmid-transfected COS-7 cells were maintained in Dulbecco's modified Eagle's medium supplemented with 10% FBS. IAVs [A/WSN/33 (H1N1), A/Memphis/1/71 (H3N2), and A/duck/313/4/78 (H5N3)] were propagated in 10-day-old embryonated hen's eggs for 2 days at 34°C and were purified by sucrose density gradient centrifugation as described previously (36).

Antibodies. Mouse antisulfatide MAb (GS-5; immunoglobulin M [IgM]) (5, 33, 39) and mouse antiglycosphingolipid, Gb_3Cer MAb (TU-1; IgM) were prepared as described previously (14, 20, 33). Mouse anti-NP (4E6), anti-H3 HA (2E10 and 1F8), and anti-N2 NA (SI-4) MAbs (IgG) were established by a procedure described previously (20) using influenza virus A/Memphis/1/71 (H3N2) and A/Japan/305/57 (H2N2) strains. In experiments on virus infection and replication, each MAb was used in the supernatant of each mouse hybridoma cultured with a serum-free medium, Hybridoma-SFM (Invitrogen Corp., Carlsbad, CA).

Cloning and transfection. Total RNA of cells was extracted with the TRIzol reagent (Invitrogen Corp., Carlsbad, CA) and was converted to cDNA by using a TaKaRa RNA PCR kit (avian myeloblastosis virus), version 3.0 (Takara Bio Inc., Shiga, Japan). The *CGT* and *CST* genes from MDCK cells were determined using a 3′-Full RACE Core set (Takara Bio Inc., Shiga, Japan) and a 5′-Full RACE Core set (Takara Bio Inc., Shiga, Japan). We obtained two patterns of open reading frame (ORF) sequence for the *CST* mRNA from MDCK cells. One had the same number of base pairs as the human *CST* ORF, but the other had an insertion of 3 bp between positions 131 and 132 relative to the start codon. The *CST* gene was amplified with PCR primers 5′-CGGAATTCCGATGCCG CTGCCGCAGAAGAAGC-3′ and 5′-CCGGAATTCCGGTCACCACCTCA GAAAGTCCCGGATGA-3′, containing an EcoRI site using *pfuUltra* high-fidelity DNA polymerase (Stratagene, CA). Two pGEM-CST vectors containing no insertion or a three-base insertion in the *CST* gene were generated by insertion of the PCR fragment of the *CST* gene treated with EcoRI into the EcoRI site of the pGEM-T Easy vector (Promega, Madison, WI). The fragment of the *CST* ORF from pGEM-CST treated with EcoRI was inserted into the EcoRI site of the pIRES-neo vector (BD Biosciences, CA). The *CGT* gene was amplified with PCR primers 5′-CGGCGGCGGCGT CTCGCATGAAGTCTTACACTCCGTATTCATGC-3′ and 5′-CGGCGGCGT CTCGAATTTTTCACCTTCTTTTCATGTTTAATATGGC-3′ using *Tbr* EXT DNA polymerase (Finnzymes Oy, Finland). A pTARGET-CGT vector was generated by insertion of the PCR fragment of the *CGT* gene into the pTARGET vector (Promega, Madison, WI) by TA cloning. A PCR fragment containing two NotI sites was obtained by PCR using the pTARGET-CGT vector as a template with primers 5′-ATAAGAATGCGGCCGCTAAACTATATGAAGTCTTACA CTCCGTATTTCATGCTCCTG-3′ and 5′-ATAAGAATGCGGCCGCTAAAC TATTCATTTCACCTTCTTTTCATGTTTAA-3′. The PCR fragment of the *CGT* ORF treated with NotI was inserted into the NotI site of the pIRES-neo vector containing the *CST* ORF. Then, two bicistronic expression pIRES-CST-CGT vectors (no insertion or a three-base insertion in the *CST* gene), simultaneously expressing both the CST and CGT proteins from the same mRNA, were generated.

The *ASA* gene from HeLa cells was amplified with PCR primers 5′-GGAAT TCCATGGGGGCACCGCGGT-3′ and 5′-CGGAATTCCGTCAGGCATGG GGATCTGGGC-3′, containing an EcoRI restriction site, using *pfuUltra* high-fidelity DNA polymerase. A pGEM-ASA vector was generated by insertion of the PCR fragment into the EcoRI site of the pGEM-T Easy vector. The PCR fragment of the *ASA* ORF amplified with PCR primers 5′-CATGCCATGGGG GCACCGCGGTC-3′ (containing an NcoI restriction site) and 5′-CGGAATTC CGGGCATGGGGATCTGGGCA-3′ (containing an EcoRI restriction site and stop codon deletion due to fusion with a histidine tag) from pGEM-ASA was inserted into the region between the NcoI site and the EcoRI site of the expression pTriEx3-neo vector (Novagen, Darmstadt, Germany). A bicistronic-expression pTriEx3-ASA vector simultaneously expressing both the ASA and neomycin phosphotransferase proteins from the same mRNA was then generated. Sequences of the inserted genes in all generated plasmids were confirmed using an ABI Prism 310NT genetic analyzer (Applied Biosystems, CA).

COS-7 cells were transfected with the pIRES-CST-CGT vector (containing no insertion or a three-base insertion in the *CST* gene) using the transfection reagent TransIT-293 (Panvera, Madison, WI). The transfected cells were selected in the presence of 1 mg/ml G418 (Promega, Madison, WI) for more than 3 weeks, followed by cloning. Screening of the sulfatide-enriched cell clone was performed by observation of expression of sulfatide stained with GS-5 and fluorescein isothiocyanate (FITC)-conjugated goat anti-mouse IgM secondary antibody (Sigma-Aldrich Corp., MO) under a fluorescence microscope (Olympus IX70; Olympus, Tokyo, Japan). Two sulfatide-enriched cell clones, one of which had a three-base insertion in the *CST* gene, were generated, and stable mRNA expression of the *CST* gene derived from pIRES-CST-CGT within each cell clone was confirmed by PCR with primers 5′-AGTACTTAATACGACTCACT ATAGG-3′ (T7 promoter primer) and 5′-ACGGTGATGAAGGTGGC-3′ (*CST* antisense primer) using mRNA expression of the glyceraldehyde 3-phosphate dehydrogenase gene (*GAPDH*) as a control housekeeping gene (Fig. 2A).

MDCK cells were transfected with the pTriEx3-ASA vector using the transfection reagent TransIT-293. The transfected cells were selected in the presence of 1 mg/ml G418 for more than 3 weeks. Screening of ASA activity and sulfatide depletion in the transfected cells was performed. Sulfatase activities in 120 to 150 μg of the transfected cells were measured as described previously (43) using 4-methylumbelliferyl sulfate (Research Organics, OH). Sulfatide depletion in the transfected cells was observed by staining of sulfatide with GS-5 and FITC-conjugated goat anti-mouse IgM secondary antibody under a fluorescence microscope. Stable mRNA expression of the *ASA* gene derived from pTriEx3-ASA was confirmed by PCR with primers 5′-AGTACTTAATACGACTCACTATA GG-3′ (T7 promoter primer) and 5′-AGCCAGGACTTCGGC-3′ (*ASA* antisense primer) using mRNA expression of *GAPDH* as a control housekeeping gene (Fig. 3A).

RNAi against *CST* mRNA. cDNA sequences 5′-GCTTCAACATCATCTGC A-3′ (CST401-419, numbering from the ATG codon) or 5′-CGACTTCGACTA CCCGGCC-3′ (CST337-357) of the *CST* coding region and 5′-CTGGAGTTG TCCCAATTCT-3′ (GFP29-47) of the green fluorescent protein gene (*GFP*) coding region were inserted into the cloning site between BamHI and HindIII of the small interfering RNA (siRNA) expression vector pSilencer3.1-H1 neo (Ambion Inc., Austin, TX). MDCK cells were transfected with these vectors using TransIT-293 (Panvera, Madison, WI) and maintained in the presence of G418 (1 mg/ml) for 3 weeks. Then, G418-resistant MDCK cells were cloned in the presence of G418 (500 μg/ml). Endogenous mRNA of the *CST* gene in each MDCK clone was quantitated by quantitative real-time reverse transcription-PCR (RT-PCR) (LightCycler 2.0; Roche Applied Science, Tokyo, Japan) using the primer pairs 5′-AGCACGGGCTCAAGTTC-3′ (CST302-318) and 5′-ACG GTGATGAAGGTGGC-3′ (CST469-485), which amplify the cDNA region of *CST* containing CST401-419 and CST337-357. Endogenous mRNA of the *GAPDH* gene, as a housekeeper gene, was quantitated using the primer pairs 5′-TCAACGGATTTGGCCGTATTGG-3′ (GAPDH17-38) and 5′-TGAAGGG GTCATTGATGGCG-3′ (GAPDH97-106). The relative amount of mRNA of the *CST* gene is shown as a percentage of that in parent cells. Standard deviations were calculated from the three independent experimental data. To investigate whether RNA interference (RNAi) against the *CST* mRNA inhibits nuclear export of viral NP, SulCOS1 cells and MDCK cells were transfected with an siRNA vector, piGENE-tRNA Pur (iGENE Therapeutics, Inc., Ibaraki, Japan), in which 5′-GCTTCAACATCATCTGCAACCACATGCGCT-3′ (CST401-430) or 5′-CAACCCGCAGGTGCAGGAACACATCCTGGA-3′ (CST693-722) was inserted between SacI and KpnI sites against *CST* mRNA of MDCK cells. An siRNA vector in which the *GFP* sequence 5′-ACTGGAGTTGTCCCAATTCT TGTTGAATTA-3′ was inserted was used as a negative control. The transfected cells were maintained in a serum-free medium for 3 days at 37°C and infected with IAV at a high multiplicity of infection (MOI). After 7 h at 34°C, the infected cells were fixed with cold methanol and stained by 4′,6′-diamidino-

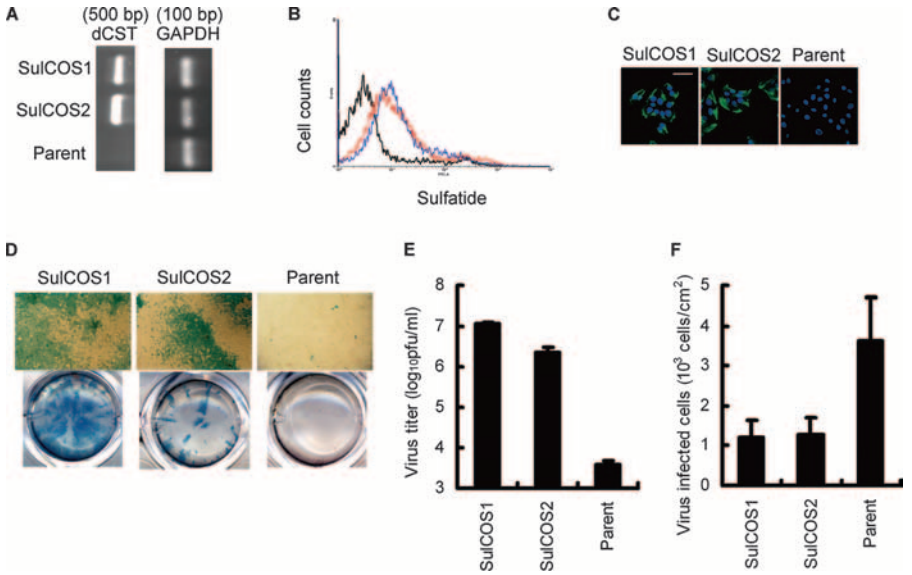

FIG. 2. Multiple replications of IAV in sulfatide-enriched COS-7 cells. Two sulfatide-enriched cell clones were generated by transfection of COS-7 cells with both dog *CST* (dCST) and *CGT* genes and cloning. (A) Detection of dCST mRNA expression in sulfatide-enriched cell clones (SulCOS1 and SulCOS2) by RT-PCR. *GAPDH* mRNA was used as a control. (B) Flow cytometry analysis of sulfatide contents on the surface of sulfatide-enriched cell clones (SulCOS1, red line; SulCOS2, blue line) and parent cells (black line) with antisulfatide MAb (GS-5). (C) Fluorescence observation of sulfatide (green) and nucleus (blue) in sulfatide-enriched cell clones and parent cells. Scale bar = 50 μm. (D) Observation of infected cells in a well (lower) or under an optical microscope at magnification ×40 (upper) at 24 h postinfection in the presence of acetylated trypsin to generate multiple virus replications. Cells were infected with A/WSN/33 (H1N1) at 2.5×10^2 PFU per well. (E) Virus multiple replication titers in the supernatant from infected cells of panel D were measured by a plaque assay. (F) The number of initial infection in sulfatide-enriched cells. Sulfatide-enriched cells and parent cells were infected with IAV at 1.25×10^4 PFU per well. At 15 h postinfection in the presence of zanamivir to prevent virus multiple replications, the infected cells were counted per area unit. Standard deviations were calculated from the three independent experimental data.

2-phenylindole dihydrochloride (DAPI), GS-5, and anti-NP (4E6). The stained cells were observed under an LSM 510 confocal microscope (Carl Zeiss Inc., Thornwood, NY).

Virus infection and multiple replications. Cells were seeded in a 24-well plate (0.5×10^5 cells/well). Cells were infected with IAV strain A/WSN/33 (H1N1) sustained in a serum-free medium at 34°C for 1 h. To examine initiation of infection of IAV, infected cells were maintained in a serum-free medium containing zanamivir (1 μM), a specific IAV sialidase inhibitor, to prevent multiple viral replications. To evaluate multiple viral replications, infected cells were maintained in 500 μl of a serum-free medium without any antibodies or with GS-5 (300 μg/ml) or TU-1 (500 μg/ml) at 37°C in the presence of acetylated trypsin (2.5 μg/ml), which cleaves viral HA to the HA1 and HA2 subunits, in order to activate viral fusion activity, which is required for multiple virus replications. The infected cells were fixed with cold methanol for 30 s, and they were incubated with anti-NP MAb (4E6) for 30 min and then with horseradish peroxidase-conjugated goat anti-mouse IgG plus IgM (Jackson Immuno Research, West Grove, PA) for 30 min at room temperature. Viral NPs within the infected cells were developed by addition of H_2O_2, *N,N*-diethyl-*p*-phenylenediamine dihydrochloride, and 4-chloro-1-naphthol as described previously (36). Titers of progeny virus in the supernatant from infected cells were measured by a plaque assay. All pictures were taken by using an Olympus DP70 or C5050 camera.

Plaque assay and virus titration. For quantitation of virus titers, confluent monolayer MDCK cells were incubated with log dilutions of the virus in a serum-free medium for 1 h at 34°C. The infected monolayers were then overlaid with a solution of a serum-free medium containing acetylated trypsin (2.5 μg/ml) and 0.8% agarose. The monolayers were incubated for 2 to 3 days at 34°C until plaques could be visualized. Standard deviations were calculated from the three independent experimental data.

Fluorescence-activated cell sorter analysis of sulfatide. MDCK cells, sulfatide knockdown MDCK cells, COS-7 cells, and sulfatide-enriched COS-7 cell clones (0.5×10^5 cells/well in a 24-well plate) were maintained in a serum-free medium, Hybridoma-SFM, for 2 days at 37°C and were harvested with treatment of 0.125% trypsin. The cells were fixed with 3% paraformaldehyde for 30 s, and they were incubated in the medium containing GS-5 for 1 h on ice and then with FITC-conjugated goat anti-mouse IgM antibody (Sigma-Aldrich Corp., MO) for 1 h on ice. Fluorescence for cells was excited with the 488-nm line of an argon laser on a fluorescence-activated cell sorter Canto II flow cytometer (BD, Franklin Lakes, NJ). At least 1×10^4 cells were analyzed for each sample.

Fluorescence microscopy. To visualize sulfatide expression in cells, cells grown on glass coverslips (Teflon printed glass slides; Erie Scientific Company, Portsmouth, NH) were fixed and permeabilized with cold methanol for 30 s, incubated with GS-5, and then incubated with FITC-conjugated goat anti-mouse IgM secondary antibody. To visualize distribution of viral NP, HA, or NA within infected cells, cells were infected with IAV strain A/Memphis/1/71 (H3N2) at an MOI of 5 PFU per cell for 1 h at 34°C and maintained in a medium supplemented with 1% FBS at 37°C. At 7 h postinfection, the infected cells were fixed and permeabilized with cold methanol for 30 s. The infected cells were incubated with mouse anti-NP (4E6), anti-H3 HA (2E10), or anti-N2 NA (SI-4) MAb and then with tetramethyl rhodamine-conjugated goat anti-mouse IgG secondary antibody (Sigma-Aldrich Corp., MO). Nuclei were visualized with DAPI (Dojindo Laboratories, Kumamoto, Japan). The cells were observed under a confocal microscope. To evaluate nuclear localization of NP in sulfatide-enriched or knockdown cells, pictures (magnification, ×400) with staining of NP and nuclei were taken at 5.5 and 6.5 h postinfection at 34°C. Cells in which most of the NP was localized in the nucleus were counted in least six fields per cell line. Nuclear localization of NP in each cell line was expressed as the ratio of cells with nuclear localization of NP to total infected cells.

Inhibition of IAV binding to sulfatide by MAbs. Five hundred picomoles of sulfatide was immobilized in wells of microtiter plates (F96 Polysorp; Nunc, Roskilde, Denmark) as described previously (37). Each well was blocked by 0.2% bovine serum albumin containing 0.1% (wt/vol) MEGA-10 (Dojindo Laboratories, Mashiki, Japan) at 4°C overnight. For the binding inhibition test of anti-IAV MAbs (2E10, 1F8, and SI-4), 50 μl of influenza virus A/Memphis/1/71 (H3N2) suspension (24 hemagglutinating units) was treated with 50 μl of each anti-IAV MAb at 4°C for 2 h. The reaction mixtures were added to the well and incubated at 4°C for 2 h. For the binding inhibition test of anti-glycolipid MAbs (GS-5 and TU-1), 50 μl of each MAb was added to the wells. After a 2-h incubation at 4°C, 50 μl of IAV suspension (24 hemagglutinating units) was added to the wells and incubated at 4°C for 2 h. Binding of virus to sulfatide was detected by using rabbit

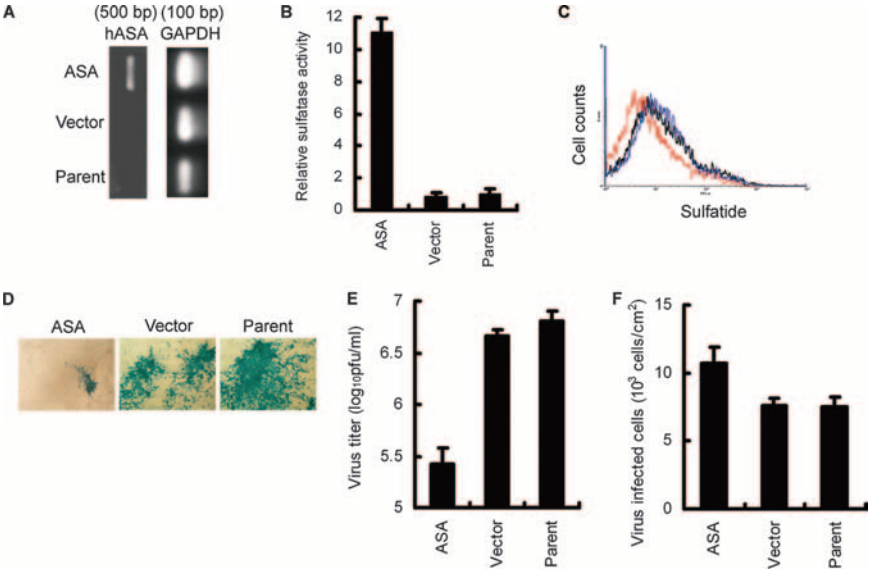

FIG. 3. Decreased multiple replications of IAV in sulfatide knockdown MDCK cells. Sulfatide knockdown cells (*ASA*) were generated by transfection of MDCK cells (Parent) with the human *ASA* gene (hASA) and cultured in the presence of G418 for more than 3 weeks. As a control, G418-resistant MDCK cells transfected with an empty vector (Vector) were also used. (A) Detection of hASA mRNA expression in sulfatide knockdown cells by RT-PCR. *GAPDH* mRNA was used as a control. (B) Increased sulfatase activity of sulfatide knockdown cells. (C) Flow cytometry analysis of sulfatide contents on the surface of sulfatide knockdown cells (*ASA*, red line) and control cells (Vector, blue line; Parent, black line) stained with GS-5. (D) Observation of infected cells under an optical microscope at magnification ×40 at 26 h postinfection in the presence of acetylated trypsin. Cells were infected with A/WSN/33 (H1N1) at 2.5×10^1 PFU per well. (E) Virus multiple replication titers in the supernatant from infected cells of panel D were measured by a plaque assay. (F) The number for initial infection in sulfatide-knockdown cells. The cells were infected with IAV at 1.25×10^4 PFU per well. At 16 h postinfection in the presence of zanamivir, the infected cells were counted per area unit. Standard deviations were calculated from the three independent experimental data.

anti-IAV polyclonal antibody and horseradish peroxidase-conjugated protein A as described previously (37).

in vivo antiviral assay. Female C57BL/6 mice (8 weeks) were infected intranasally with 20 μl of a 4×10^3 50% tissue culture infective dose of mouse-adapted IAV A/WSN/33 (H1N1). Twenty-five microliters of phosphate-buffered saline containing GS-5 (300 μg/ml) was administered intranasally once daily for 5 days beginning 1 day preinfection. Four mice per group were monitored for body weight and mortality daily for 7 days after infection until all mice had succumbed to infection or were recovering as assessed by body weight. Lung histopathology was examined on day 6 after IAV infection.

Nucleotide sequence accession numbers. Nucleotide sequence data for the dog *CST* genes are available in GenBank under accession numbers 240641 and 240642.

RESULTS

Sulfatide-enriched COS-7 cells remarkably promote IAV multiple replications. To determine whether sulfatide contributes to the IAV life cycle, we genetically produced sulfatide-enriched cells from parental COS cells defective in sulfatide (10, 25). It has been suggested that sulfatide accumulation leads to a feedback inhibition of galactosylceramide synthesis (30). We therefore obtained both *CST* and *CGT* genes from MDCK cells by PCR cloning methods. COS-7 cells were transfected with the expression pIRES-neo vector containing an internal ribosome entry site between the *CST* gene and the CGT gene (Fig. 2A). We established two cell clones (SulCOS1 and SulCOS2) that stably express sulfatide by cloning in the presence of neomycin and demonstrated sulfatide expression by flow cytometry (Fig. 2B) and immunofluorescence microscopy (Fig. 2C) with GS-5.

Surprisingly, obvious enhancement of IAV multiple replications in sulfatide-enriched cells was confirmed by immunostaining of the cells (Fig. 2D). Titers of progeny virus in the supernatant from cell clones increased by 500 to 3,000 times in comparison with results for that from the parent COS-7 cells, which showed little replication of IAV (Fig. 2E). In contrast, sulfatide-enriched cells showed a reduction of about 28% in the initial infection in comparison with that of the parent cells (Fig. 2F). Although sulfatide binds to IAV, it may not be important for initial IAV infection as a virus receptor. It is thought that excessive sulfatide competitively inhibits initial virus binding to actual receptors (sialoglycoconjugates). Also, abnormal sulfatide storage due to ASA deficiency is known to cause down-regulation and mistargeting of cellular proteins, such as the lipid raft-associated protein MAL (29). An excessive amount of sulfatide may inhibit normal functions in the initial IAV phase, such as endocytosis.

Sulfatide knockdown MDCK cells show significant reduction in IAV multiple replications. To evaluate the impact of sulfatide depletion on IAV replication, we generated sulfatide knockdown cells from MDCK cells by transfection with the *ASA* gene and by RNAi targeting *CST* mRNA. We obtained MDCK cells stably expressing the *ASA* gene in the presence of neomycin after transfection with the expression pTriEx3-neo vector containing the internal ribosome entry site between the *ASA* gene and the neomycin resistance gene, simultaneously expressing both the ASA protein and the neomycin phosphotransferase from the same mRNA (Fig. 3A). Stable expression of the *ASA* gene led to an approximately 11-fold increase in sulfatase activity compared to that of parent cells or cells

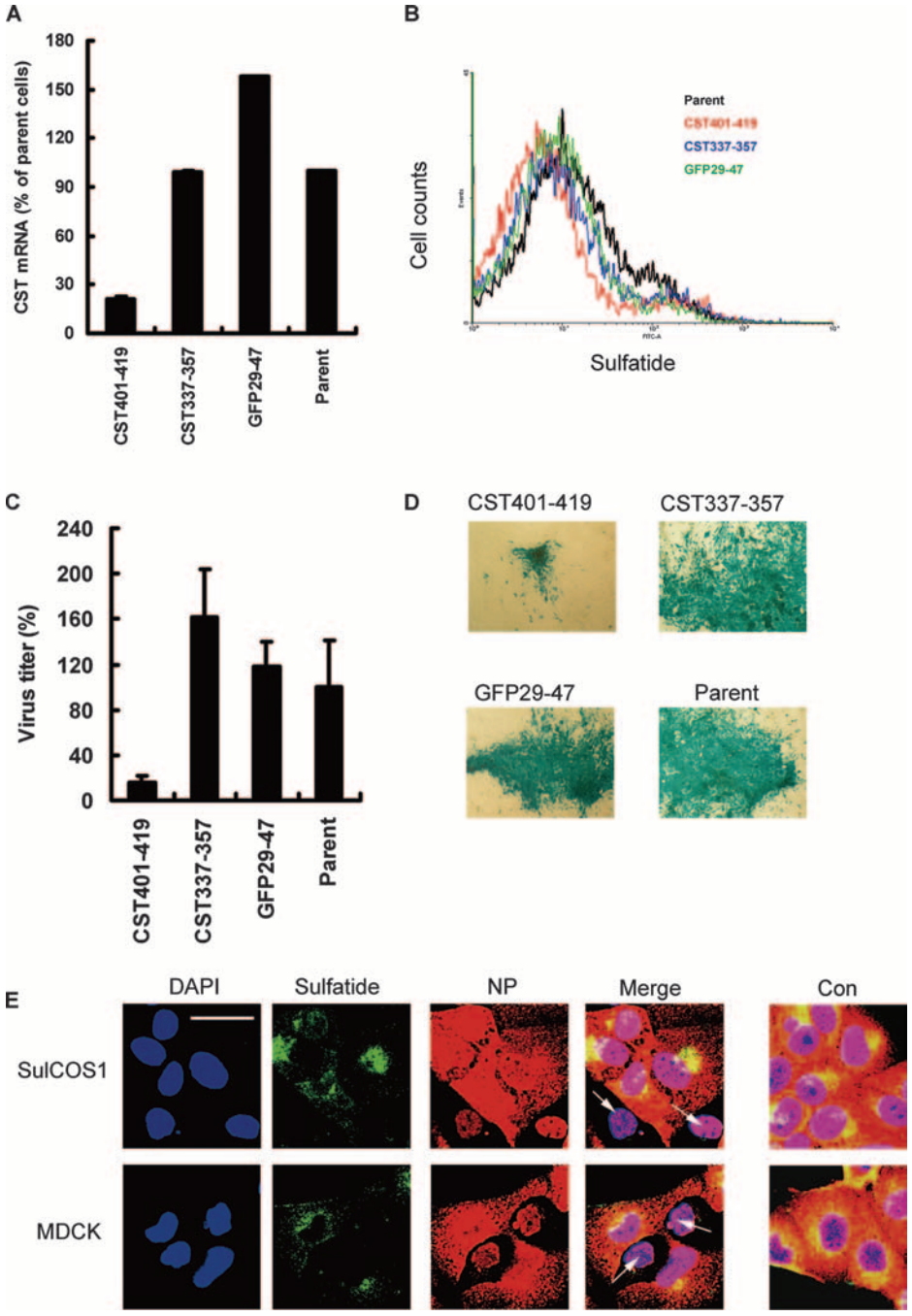

FIG. 4. Decreased multiple replications of IAV in sulfatide knockdown MDCK cells transfected with an siRNA vector against mRNA of the *CST* gene. (A) Endogenous mRNA of the *CST* gene in MDCK cells was quantitated by quantitative real-time RT-PCR. Endogenous mRNA of the *GAPDH* gene, as a housekeeper gene, was quantitated. The relative amount of mRNA of the *CST* gene is shown as a percentage of that in parent cells. (B) Flow cytometry analysis of sulfatide contents on the surface of transfected cells (CST401-419, red line; CST337-357, blue line; GFP29-47, green line) and parent cells (black line) with GS-5. (C) The cells were infected with A/WSN/33 (H1N1) at 5×10^1 PFU per well. At 26 h postinfection in the presence of acetylated trypsin, multiple replication titers of virus in supernatants from infected cells were measured by a plaque assay. (D) Observation of the infected cells analyzed in panel C under an optical microscope at magnification ×40. (E) Inhibition of nuclear export of viral NP by RNAi against *CST*. SulCOS1 cells (upper) or MDCK cells (lower) were transfected with an siRNA vector against *CST* mRNA of MDCK cells. A vector with the *GFP* sequence inserted was used as a negative control (Con). The infected cells were fixed with cold methanol and stained by DAPI (blue), GS-5 (green), and 4E6 (red). The stained cells were observed under a confocal microscopy. Scale bar = 20 μm. The arrowheads show sulfatide knockdown cells.

transfected with an empty vector alone (Fig. 3B). The effect of sulfatide knockdown in these cells was confirmed by flow cytometry (Fig. 3C) with antisulfatide MAb (GS-5) (15, 33).

ASA activation is known to be required for association of ASA with sphingolipid activator protein 1 (SAP-1) (4, 27); however, ASA activation in MDCK cells did not require expression of the exogenous SAP-1 gene. MDCK cells may express a large amount of endogenous SAP-1. We assessed initial

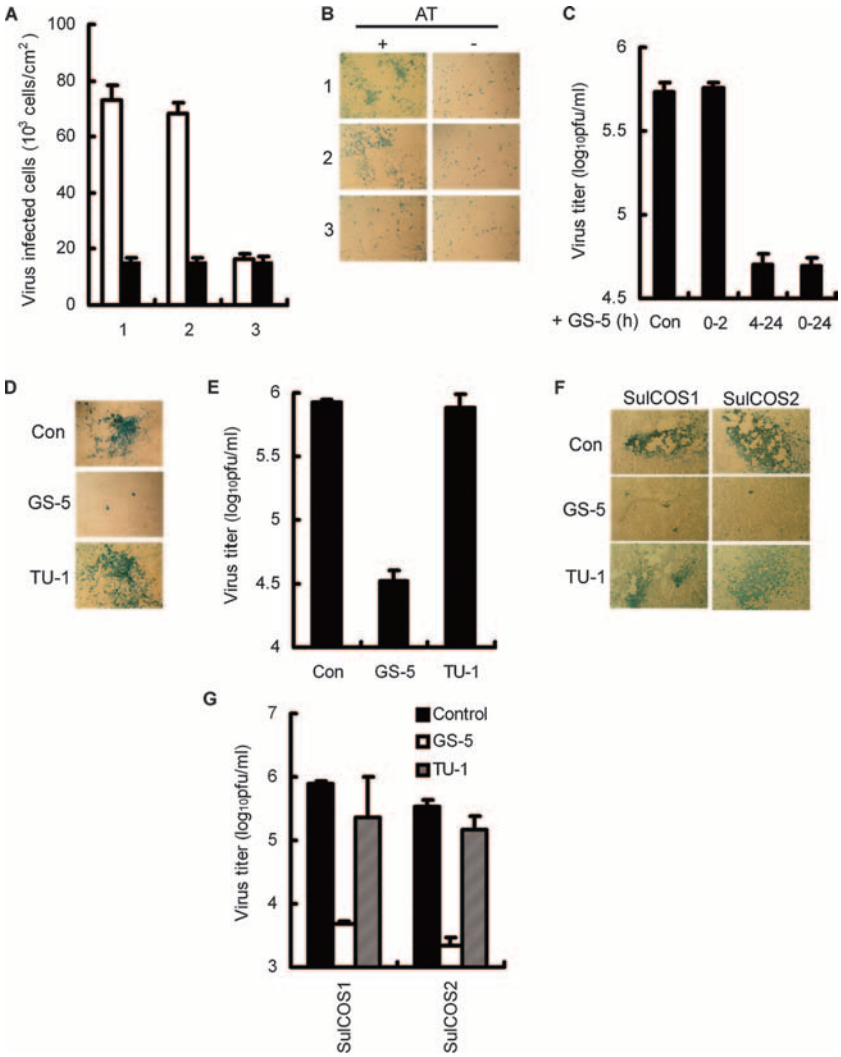

FIG. 5. Decreased multiple replications of IAV in MDCK cells or sulfatide-enriched COS-7 cells treated with GS-5. (A) 1, MDCK cells were incubated with a medium containing GS-5 at 37°C for 30 min before infection; 2, the cells were infected with an A/WSN/33 (H1N1) suspension containing GS-5 at 37°C for 1 h. 3, The cells were maintained in a medium containing GS-5 at 34°C after infection. In all cases, the cells were infected with IAV at 2.5×10^4 PFU per well. At 15 h postinfection in the presence (open bars) or the absence (solid bars) of acetylated trypsin (AT), the number of infected cells per area unit was determined. (B) Observation under an optical microscope at magnification ×40 of infected cells analyzed in panel A. (C) MDCK cells were infected with IAV at 2.5×10^1 PFU per well. The infected cells were maintained in a medium containing GS-5 plus AT for indicated times after virus infection. At 24 h postinfection, infectious progeny virus titers in the supernatant from infected cells were measured by a plaque assay. (D) Observation of the infected MDCK cells treated with GS-5 under an optical microscope at magnification ×40 at 26 h postinfection. The cells were infected with IAV at 2.5×10^1 PFU per well and then maintained in a medium without any antibodies (Con) or containing GS-5 or anti-Gb_3Cer MAb (TU-1) plus AT as described for panel C. (E) Multiple replication titers of virus in the supernatant from infected cells shown in panel D were measured by plaque assay. (F) Observation of sulfatide-enriched cells (SulCOS1 and SulCOS2) treated with GS-5 under an optical microscope at magnification ×40. The cells were infected with IAV at 2.5×10^2 PFU per well, maintained in a medium containing GS-5 or TU-1 plus AT, and stained at 20 h postinfection. (G) Multiple replication titers of virus in the supernatant from the infected cells shown in panel F were measured by plaque assay. Standard deviations were calculated from the three independent experimental data.

infection and replication of IAV in sulfatide knockdown MDCK cells by immunostaining for virus antigen and by a plaque assay in the presence or absence of the NA inhibitor zanamivir. Obvious reduction of IAV multiple replications in sulfatide knockdown cells was observed by immunostaining of the cells (Fig. 3D). The sulfatide knockdown cells showed an approximately 60-fold reduction in titers of progeny virus generated by IAV replication (Fig. 3E) and a slight increase in initial infection (Fig. 3F) compared to those of the parent cells.

Other sulfatide knockdown MDCK cells were generated by transfection with an siRNA expression pSilencer 3.0-H1 neo vector targeting *CST* mRNA. The effect of sulfatide knockdown in the cells was evaluated by quantitation of *CST* mRNA and sulfatide expression using quantitative real-time PCR (Fig. 4A) and flow cytometry (Fig. 4B). Application of RNAi targeting endogenous *CST* mRNA to MDCK cells also showed a variable degree of knockdown efficiency, but RNAi with siRNA of *GFP*, which was used as a control, exhibited no

reduction of IAV replication (Fig. 4C and D). Sulfatide-enriched cell clones also increased replication of other IAV strains regardless of viral subtype or host (data not shown). Taken together, the results obtained from both COS-7 cells and MDCK cells indicate that sulfatide expression in mammalian cells greatly enhances IAV multiple replications.

Antisulfatide MAb specifically inhibits IAV multiple replications but not initial infection. To determine whether an antisulfatide MAb has an inhibitory effect on IAV infection, MDCK cells were treated with GS-5 before, at the same time as, and after the virus infection. Treatment with GS-5 after IAV infection induced a great reduction in IAV multiple replications, but GS-5 treatment before and at the same time as IAV infection had no effect on viral initial infection and replication (Fig. 5A and B). Additionally, GS-5 treatment induced distinct inhibition of IAV replication for 4 to 24 h but not for 0 to 2 h after IAV infection (Fig. 5C). In contrast, an antiglycosphingolipid, Gb_3Cer MAb (TU-1), which was also enriched in lipid rafts (20), exhibited no inhibition of IAV replication under similar conditions (Fig. 5D and E). GS-5 also had the same effect on other strains independently of viral subtype and host (data not shown). Similarly, sulfatide-enriched cells that were treated with GS-5 after virus infection showed a great reduction in IAV replication, as determined by measuring the titers of progeny virus of the supernatant and by microscopic observation (Fig. 5F and G).

Sulfatide promotes formation and release of the infectious progeny virus. To determine the requirement of sulfatide for formation of infectious progeny virus from virus-infected cells, sulfatide-enriched cell clones and sulfatide knockdown MDCK cells were infected with IAV at a high MOI, and then progeny virus titers in the supernatant were determined by plaque assays. The sulfatide-enriched cell clones showed about a 50- to 100-times increase (Fig. 6A) and the sulfatide knockdown cells showed about a 60% decrease in formation and release of the infectious progeny virus compared with that of the control cells (Fig. 6C). Similarly, treatment of virus-infected MDCK cells and sulfatide-enriched cells with GS-5 but not with TU-1 resulted in a significant decrease in formation and release of the infectious progeny virus (Fig. 6B and D).

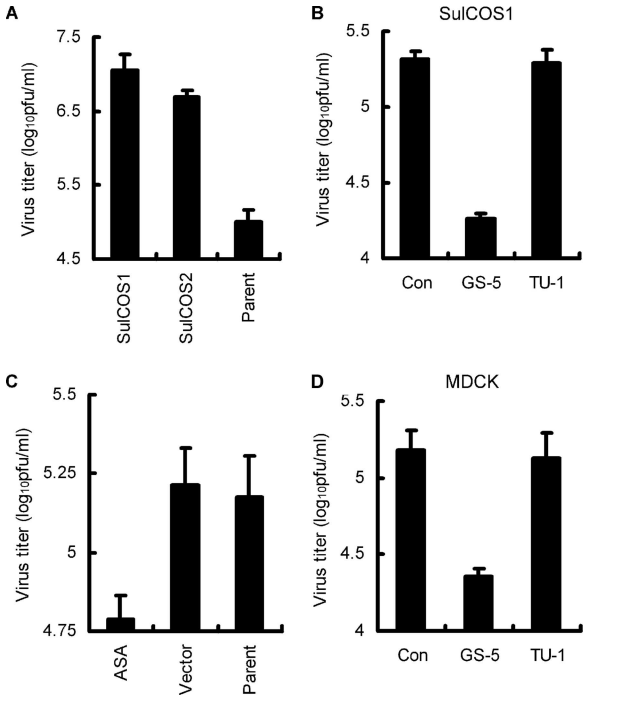

FIG. 6. Efficiency of formation of infectious progeny viruses from sulfatide-enriched COS-7 cells or sulfatide knockdown MDCK cells. Cells were infected with A/WSN/33 (H1N1) at a high MOI (1 PFU per cell) and maintained in the absence of acetylated trypsin to prevent multiple viral replications. Supernatants from infected cells were incubated with AT (10 μg/ml) at 37°C for 30 min in order to activate infectivity of the harvested progeny virus. Then, infectious progeny virus titers in the supernatant were measured by a plaque assay. (A) Infectious progeny virus titers from sulfatide-enriched COS-7 cell clones (SulCOS1 and SulCOS2) and parent cells (Parent) at 20 h postinfection. (B) Infectious progeny virus titers from infected SulCOS1 cells maintained in a medium containing GS-5 or TU-1 for 16 h. As a control, a medium without any antibodies (Con) was used. (C) Infectious progeny virus titers from sulfatide knockdown MDCK cells (ASA) and parent cells (Parent) at 16 h postinfection. As a control, G418-resistant MDCK cells transfected with an empty vector (Vector) were used. (D) Infectious progeny virus titers from infected MDCK cells maintained in a medium containing GS-5 or TU-1 for 16 h. Standard deviations were calculated from the three independent experimental data.

Sulfatide on the cell surface promotes translocation of newly synthesized viral NP from nucleus to cytoplasm. NP of IAV forms viral ribonucleoprotein (vRNP) complexes together with the viral polymerase (PB1, PB2, and PA) and viral genome RNA segments in the nucleus, and the vRNP complexes are then exported to the cytoplasm, while two surface spike glycoproteins, HA and NA, which possess apical sorting signals, are transported to the plasma membrane via the exocytic pathway (18, 21). We examined by immunofluorescence microscopy the intracellular distribution of the newly synthesized viral NP, HA, and NA in parent cells and sulfatide-enriched cell clones infected with IAV.

In the sulfatide-enriched cells at 7 h after infection, most newly synthesized HA and NA localized to the cell surface (Fig. 7A and B), and most newly synthesized viral NP translocated from the nucleus to the cytoplasm (Fig. 7C). In the parent cells, most newly synthesized viral HA and NA localized to the cell surface (Fig. 7D and E), but most newly synthesized viral NP remained in the nucleus (Fig. 7F). Interestingly, in sulfatide-enriched cells that were treated with GS-5 but not with TU-1 after IAV infection, most newly synthesized viral NP remained in the nucleus (Fig. 7I and J) despite normal localization of newly synthesized viral HA (Fig. 7G and H). Delayed translocation of newly synthesized viral NP from the nucleus to the cytoplasm was observed in sulfatide knockdown MDCK or SulCOS1 cells transfected with the RNAi vector against *CST* mRNA, but there was NP distribution in the cytoplasm of cells in which sulfatide was clearly detected (Fig. 4E). Similarly, in both sulfatide knockdown MDCK cells and MDCK cells treated with GS-5 but not with TU-1 after IAV infection, most newly synthesized viral NP remained in the nucleus (data not shown). In addition, we quantitatively evaluated nuclear localization of NP in sulfatide-enriched cells and sulfatide knockdown cells. Nuclear localization of NP in each cell line was calculated as a percentage of total infected cells with nuclear localization of NP. Translocation of NP from the nucleus to the cytosol in sulfatide-enriched cells was increased

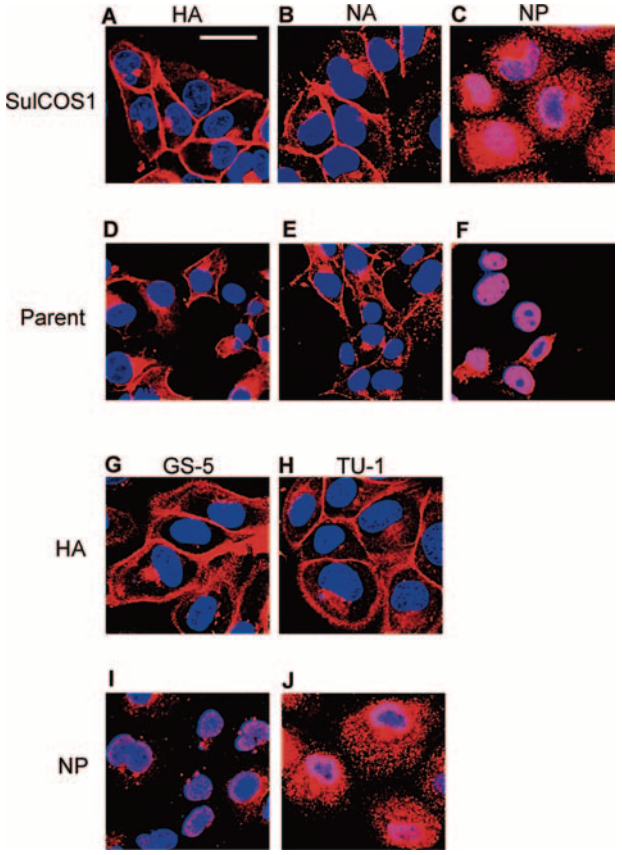

FIG. 7. Distribution of viral HA, NA, and NP in infected sulfatide-enriched COS-7 cells or parent cells and in infected sulfatide-enriched cells treated with GS-5. SulCOS1 and parent cells were infected with IAV A/Memphis/1/71 (H3N2) at an MOI of 5 PFU per cell and maintained in a medium containing 1% FBS or containing GS-5 or TU-1 plus 1% FBS at 37°C. At 7 h postinfection, the infected cells were fixed. The newly synthesized viral proteins, HA, NA, and NP, were stained with respective specific MAbs (red). Nuclei within the cells were stained with DAPI (blue). Scale bar = 50 μm. (A to C) Distribution of HA (A), NA (B), or NP (C) in infected SulCOS1 cells. (D to F) Distribution of HA (D), NA (E), or NP (F) in infected parent cells. (G to J) Distribution of HA (G and H) or NP (I and J) in infected SulCOS1 cells treated with GS-5 (G and I) or TU-1 (H and J).

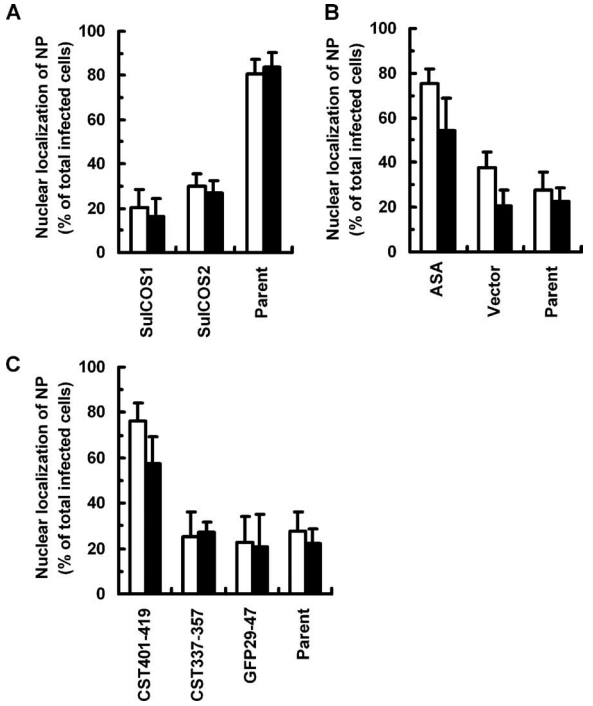

FIG. 8. Nuclear localization of NP in sulfatide-enriched and sulfatide knockdown cells. At 5.5 h (open columns) or 6.5 h (filled columns) postinfection, nuclear localization of NP in sulfatide-enriched cells (A) or sulfatide-knockdown cells by ASA overexpression (B) or RNAi against *CST* mRNA (C) was observed under a confocal microscope at magnification ×400. Cells in which most of the NP was localized in the nucleus were counted. Nuclear localization of NP in each cell line was expressed as a percentage of total infected cells with nuclear localization of NP. Standard deviations were calculated from at least six fields per cell line.

compared to that in parent cells (Fig. 8A), whereas nuclear localization of NP in sulfatide knockdown cells was more than that in parent cells or control cells (Fig. 8B and C). The results suggest that sulfatide, which is expressed on the cell surface in the process of IAV replication, promotes nuclear export of vRNPs.

Association of sulfatide with HA delivered to the cell surface induces translocation of newly synthesized NP from nucleus to cytoplasm. We previously found that sulfatide bound to IAV particles and inhibited viral infection and also inhibited viral sialidase activity under low-pH conditions (36, 38). Influenza virus HA and NA are known to cluster in lipid rafts for assembly and budding of IAV (31, 44). To elucidate the involvement of HA and NA in the nuclear export of the viral NP regulated by sulfatide, SulCOS1 cells infected with IAV A/Memphis/1/71 (H3N2) were treated with anti-H3 HA MAb (2E10), which blocks the binding of IAV and sulfatide (Fig. 9B and C). Interestingly, translocation of the newly synthesized NP from the nucleus to the cytoplasm in the cells was almost completely suppressed by 2E10, similar to the effect of GS-5 (Fig. 9A). In contrast, anti-H3 HA MAb (1F8), which does not block the binding of IAV to sulfatide, and anti-N2 NA MAb (SI-4), as well as TU-1, did not suppress nuclear export of the viral NP. 2E10 shows hemagglutination inhibitory activity, but 1F8 does not. When 2E10 binds to the HA protein, it is thought that HA binding to the receptor is inhibited by antibody binding in the vicinity of the receptor binding pocket or by conformational change in the HA protein by pressure of antibody binding. In the former case, sulfatide may bind close to the receptor binding pocket on the HA protein, whereas in the latter case, the sulfatide association site may be a location that is subjected to conformational change by 2E10 binding. These results indicate that association of sulfatide with HA delivered to the cell surface induces translocation of the newly synthesized viral NP from the nucleus to the cytoplasm.

Antisulfatide MAb treatment protects mice from lethal IAV challenge. For assessment of whether the antisulfatide antibody can inhibit virus replication in vivo, C57BL/6 mice were intranasally infected with pathogenic influenza A/WSN/33 (H1N1) virus. GS-5 was administered intranasally once daily for 5 days beginning 1 day preinfection. The percentage of initial body weight, Kaplan-Meier survival curve, and virus

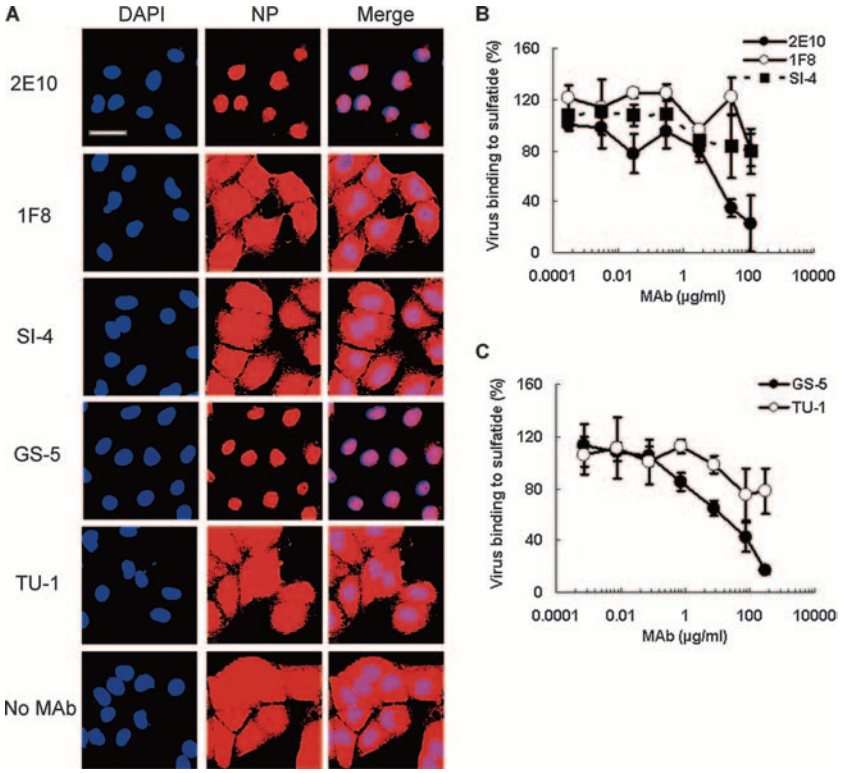

FIG. 9. Inhibition of nuclear export of the viral NP by anti-HA MAb (2E10). (A) SulCOS1 cells grown on glass coverslips were infected with A/Memphis/1/71 (H3N2) at an MOI of 1 to 2 cells/PFU for 30 min at 37°C. The infected cells were washed with PBS and maintained in 100 μl of a medium containing each anti-IAV MAb (120 μg/ml) supplemented with 1% FBS. At 6 h postinfection, the cells were fixed and permeabilized with cold methanol for 30 s. As positive and negative controls, a medium containing GS-5 or TU-1 was used. The viral NP (red) was detected with 4E6. Nuclei within the cells were stained with DAPI (blue). Scale bar = 50 μm. (B) For the inhibition assay of IAV binding to sulfatide by MAbs, IAV was treated with each anti-IAV MAb (2E10, 1F8, and SI-4) at 4°C for 2 h. The reaction mixtures were added to sulfatide-coated wells and incubated at 4°C for 2 h. (C) Each antiglycolipid MAb (GS-5 and TU-1) was added to sulfatide-coated wells. After a 2-h incubation at 4°C, IAV suspension was added to the wells and incubated at 4°C for 2 h. Virus binding to sulfatide was detected by using rabbit anti-IAV polyclonal antibody.

titers in lung homogenates of mice 4 days later were determined. The average of infectious virus titers in lung tissue homogenates of mice administered GS-5 was lower by about 17 times than that in lung tissue homogenates of control mice. Administration of GS-5 protected mice against lethal challenge with pathogenic IAV and markedly reduced progeny virus titers in the lungs of the mice (Fig. 10).

DISCUSSION

Influenza virus HA and NA are known to associate with lipid rafts for assembly and budding of IAV (31, 44). Accumulation of IAV HA triggers nuclear export of the viral genome via protein kinase Cα-mediated activation of extracellular signal-regulated kinase signaling (17). However, mechanisms by which HA accumulation regulates cell signaling remain unknown. Sulfatide is ubiquitously detected in various epithelial cell lines and animal tissues that permit sufficient IAV replication (6, 8, 10, 23, 24). Sulfatide is also enriched in lipid rafts of plasma membranes (3, 26). Sulfatide binds to IAV particles and inhibits viral sialidase activity under low-pH conditions (36, 38). In this study, we demonstrated that sulfatide is a critical component of host cells for effective production of progeny viruses by using genetically produced sulfatide knock-

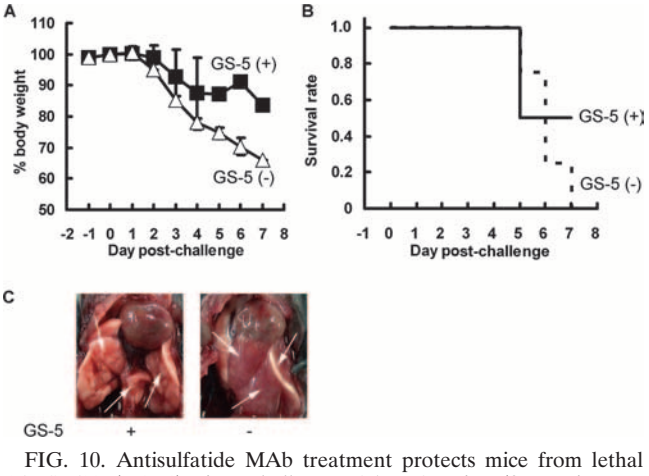

FIG. 10. Antisulfatide MAb treatment protects mice from lethal A/WSN/33 (H1N1) virus challenge. C57BL/6 mice (four mice per group) were challenged with IAV A/WSN/33 (H1N1). GS-5 was administered intranasally once daily for 5 days beginning 1 day preinfection. The percentage of initial body weight (A) and survival curve determined by the Kaplan-Meier method (B) or lung image of a live mouse at 6 days postinfection (C) is shown. At 4 days postinfection, the average of infectious virus titers (log[PFU/g of lung tissue weight]) in lung tissue homogenates administered with or without GS-5 was 1.66 or 2.90, respectively. The arrowheads in panel C show lungs. The lungs of a live mouse without GS-5 were strikingly inflamed.

down or enriched cells. Translocation of the newly synthesized NP from the nucleus to the cytoplasm in the cells was also suppressed by anti-H3 HA MAb as well as antisulfatide MAb, which blocks the binding of IAV and sulfatide. In contrast, anti-H3 HA MAb, which does not block the binding of IAV to sulfatide, and anti-N2 NA MAb as well as anti-Gb_3Cer MAb did not inhibit nuclear export of the viral NP. In addition, GM3 is abundantly detected in lipid rafts and is known to play a major role in various signal transductions through a GM3-enriched microdomain (11, 19, 41), but anti-GM3 MAb showed no inhibitory effect on IAV replication (data not shown). Overall, our data show that sulfatide regulates translocation of newly synthesized vRNP complexes from the nucleus to the cytoplasm by association with HA delivered to the cell surface.

Generally, many kinds of viruses, including IAV and HIV, induce apoptosis. Although virus-induced apoptosis is thought to be the initiation step of host defense prior to antigen presentation, it remains unknown whether virus-induced apoptosis works in an advantageous or disadvantageous way for the virus itself. For IAV, it has been suggested that virus-induced apoptosis via caspase-3 activation is advantageous for virus replication by promoting translocation of the newly synthesized viral NP from the nucleus to the cytoplasm (42). Therefore, we are currently investigating whether interaction of sulfatide with HA promotes virus-induced apoptosis. What is the mechanism of regulation by sulfatide in response to IAV infection? We propose the following hypotheses: (i) association of sulfatide with HA may regulate translocation of NS2 and M1, which are involved in exporting vRNP complexes from the nucleus (22, 28), or activation of some cellular proteins required for exporting vRNP complexes from the nucleus, such as HSP70, CRM1, and mitogen-activated protein kinase (9, 22, 42), and (ii) expression of HA on the cell surface membrane and virus-induced apoptosis promote translocation of nuclear NP to the cytoplasm though extracellular signal-regulated kinase activation (17) and caspase-3 activation, respectively (42). Association of sulfatide with HA may regulate apoptosis through some cellular proteins involved in the signal pathway of virus-induced apoptosis. It has recently been reported that the sulfogalactose moiety of sulfatide serves as a mimic of tyrosine phosphate (16). Tyrosine phosphate reaction plays a key role in several signal cascade pathways. This report supports the association of sulfatide with the signal pathway induced by virus infection.

Administration of antisulfatide MAb showed strongly inhibited IAV replication, even after virus infection, and protected mice against lethal challenge with IAV. The development of antiviral drugs will probably play a critical role in the next influenza pandemic. NA inhibitors are currently used for protection against and treatment of influenza. However, the emergence of drug-resistant viruses has become a serious problem. A strategy of using antisulfatide MAb for the treatment of IAV infection might be a solution in preventing the appearance of drug resistance mutants by targeting the host glycolipid essential for the IAV life cycle but not IAV.

ACKNOWLEDGMENTS

This work was supported by CREST (Japan Science and Technology Agency), the Sasakawa Scientific Research Grant from The Japan Science Society, and the Global COE Program from the Japan Society for the Promotion of Science.

REFERENCES

1. **Aruffo, A., W. Kolanus, G. Walz, P. Fredman, and B. Seed.** 1991. CD62/P-selectin recognition of myeloid and tumor cell sulfatides. Cell **67:**35–44.
2. **Chazal, N., and D. Gerlier.** 2003. Virus entry, assembly, budding, and membrane rafts. Microbiol. Mol. Biol. Rev. **67:**226–237.
3. **DeBruin, L. S., J. D. Haines, L. A. Wellhauser, G. Radeva, V. Schonmann, D. Bienzle, and G. Harauz.** 2005. Developmental partitioning of myelin basic protein into membrane microdomains. J. Neurosci. Res. **80:**211–225.
4. **Dewji, N., D. Wenger, S. Fujibayashi, M. Donoviel, F. Esch, F. Hill, and J. S. O'Brien.** 1986. Molecular cloning of the sphingolipid activator protein-1 (SAP-1), the sulfatide sulfatase activator. Biochem. Biophys. Res. Commun. **134:**989–994.
5. **Ding, Z., H. Kawashima, Y. Suzuki, T. Suzuki, P. A. Ward, and M. Miyasaka.** 1997. A sulfatide receptor distinct from L-selectin is involved in lymphocyte activation. FEBS Lett. **418:**310–314.
6. **Farooqui, A. A., and L. A. Horrocks.** 1985. On the role of sulfolipids in mammalian metabolism. Mol. Cell. Biochem. **66:**87–95.
7. **Harouse, J. M., R. G. Collman, and F. Gonzalez-Scarano.** 1995. Human immunodeficiency virus type 1 infection of SK-N-MC cells: domains of gp120 involved in entry into a CD4-negative, galactosyl ceramide/3′ sulfo-galactosyl ceramide-positive cell line. J. Virol. **69:**7383–7390.
8. **Hirahara, Y., M. Tsuda, Y. Wada, and K. Honke.** 2000. cDNA cloning, genomic cloning, and tissue-specific regulation of mouse cerebroside sulfotransferase. Eur. J. Biochem. **267:**1909–1917.
9. **Hirayama, E., H. Atagi, A. Hiraki, and J. Kim.** 2004. Heat shock protein 70 is related to thermal inhibition of nuclear export of the influenza virus ribonucleoprotein complex. J. Virol. **78:**1263–1270.
10. **Honke, K., M. Tsuda, Y. Hirahara, A. Ishii, A. Makita, and Y. Wada.** 1997. Molecular cloning and expression of cDNA encoding human 3′-phosphoadenylylsulfate: galactosylceramide 3′-sulfotransferase. J. Biol. Chem. **272:**4864–4868.
11. **Kabayama, K., T. Sato, K. Saito, N. Loberto, A. Prinetti, S. Sonnino, M. Kinjo, Y. Igarashi, and J. Inokuchi.** 2007. Dissociation of the insulin receptor and caveolin-1 complex by ganglioside GM3 in the state of insulin resistance. Proc. Natl. Acad. Sci. USA **104:**13678–13683.
12. **Kamisago, S., M. Iwamori, T. Tai, K. Mitamura, Y. Yazaki, and K. Sugano.** 1996. Role of sulfatides in adhesion of *Helicobacter pylori* to gastric cancer cells. Infect. Immun. **64:**624–628.
13. **Kapitonov, D., and R. K. Yu.** 1997. Cloning, characterization, and expression of human ceramide galactosyltransferase cDNA. Biochem. Biophys. Res. Commun. **232:**449–453.
14. **Konno, A., K. Nunogami, T. Wada, A. Yachie, Y. Suzuki, N. Takahashi, T. Suzuki, D. Miyamoto, M. Kiso, A. Hasegawa, and T. Miyawaki.** 1996. Inhibitory action of sulfatide, a putative ligand for L-selectin, on B cell proliferation and Ig production. Int. Immunol. **8:**1905–1913.
15. **Kurosawa, N., K. Kadomatsu, S. Ikematsu, S. Sakuma, T. Kimura, and T. Muramatsu.** 2000. Midkine binds specifically to sulfatide: the role of sulfatide in cell attachment to midkine-coated surfaces. Eur. J. Biochem. **267:** 344–351.
16. **Lingwood, C., M. Mylvaganam, F. Minhas, B. Binnington, D. R. Branch, and R. Pomes.** 2005. The sulfogalactose moiety of sulfoglycosphingolipids serves as a mimic of tyrosine phosphate in many recognition processes: prediction and demonstration of Src homology 2 domain/sulfogalactose binding. J. Biol. Chem. **280:**12542–12547.
17. **Marjuki, H., M. I. Alam, C. Ehrhardt, R. Wagner, O. Planz, H. D. Klenk, S. Ludwig, and S. Pleschka.** 2006. Membrane accumulation of influenza A virus hemagglutinin triggers nuclear export of the viral genome via protein kinase Cα-mediated activation of ERK signaling. J. Biol. Chem. **281:**16707–16715.
18. **Martin, K., and A. Helenius.** 1991. Nuclear transport of influenza virus ribonucleoproteins: the viral matrix protein (M1) promotes export and inhibits import. Cell **67:**117–130.
19. **Mitsuzuka, K., K. Handa, M. Satoh, Y. Arai, and S. Hakomori.** 2005. A specific microdomain ("glycosynapse 3") controls phenotypic conversion and reversion of bladder cancer cells through GM3-mediated interaction of α3β1 integrin with CD9. J. Biol. Chem. **280:**35545–35553.
20. **Miyamoto, D., T. Ueno, S. Takashima, K. Ohta, T. Miyawaki, T. Suzuki, and Y. Suzuki.** 1997. Establishment of a monoclonal antibody directed against Gb3Cer/CD77: a useful immunochemical reagent for a differentiation marker in Burkitt's lymphoma and germinal centre B cells. Glycoconj. J. **14:**379–388.
21. **Nayak, D. P., E. K. Hui, and S. Barman.** 2004. Assembly and budding of influenza virus. Virus Res. **106:**147–165.
22. **Neumann, G., M. T. Hughes, and Y. Kawaoka.** 2000. Influenza A virus NS2 protein mediates vRNP nuclear export through NES-independent interaction with hCRM1. EMBO J. **19:**6751–6758.
23. **Nimura, Y., and I. Ishizuka.** 1986. Glycosphingolipid composition of a renal cell line (MDCK) and its ouabain-resistant mutant. J. Biochem. (Tokyo) **100:**825–835.
24. **Nimura, Y., and I. Ishizuka.** 1990. Isolation and identification of nine sul-

fated glycosphingolipids containing two unique sulfated gangliosides from the African green monkey kidney cells, Verots S3, and their possible metabolic pathways. Biochim. Biophys. Acta **1052:**248–254.
25. **Ogura, K., K. Kohno, and T. Tai.** 1998. Molecular cloning of a rat brain cDNA, with homology to a tyrosine kinase substrate, that induces galactosylceramide expression in COS-7 cells. J. Neurochem. **71:**1827–1836.
26. **Ohta, K., C. Sato, T. Matsuda, M. Toriyama, W. J. Lennarz, and K. Kitajima.** 1999. Isolation and characterization of low density detergent-insoluble membrane (LD-DIM) fraction from sea urchin sperm. Biochem. Biophys. Res. Commun. **258:**616–623.
27. **Rafi, M. A., X. L. Zhang, G. DeGala, and D. A. Wenger.** 1990. Detection of a point mutation in sphingolipid activator protein-1 mRNA in patients with a variant form of metachromatic leukodystrophy. Biochem. Biophys. Res. Commun. **166:**1017–1023.
28. **Sakaguchi, A., E. Hirayama, A. Hiraki, Y. Ishida, and J. Kim.** 2003. Nuclear export of influenza viral ribonucleoprotein is temperature-dependently inhibited by dissociation of viral matrix protein. Virology **306:**244–253.
29. **Saravanan, K., N. Schaeren-Wiemers, D. Klein, R. Sandhoff, A. Schwarz, A. Yaghootfam, V. Gieselmann, and S. Franken.** 2004. Specific downregulation and mistargeting of the lipid raft-associated protein MAL in a glycolipid storage disorder. Neurobiol. Dis. **16:**396–406.
30. **Schaeren-Wiemers, N., P. van der Bijl, and M. E. Schwab.** 1995. The UDP-galactose:ceramide galactosyltransferase: expression pattern in oligodendrocytes and Schwann cells during myelination and substrate preference for hydroxyceramide. J. Neurochem. **65:**2267–2278.
31. **Scheiffele, P., M. G. Roth, and K. Simons.** 1997. Interaction of influenza virus haemagglutinin with sphingolipid-cholesterol membrane domains via its transmembrane domain. EMBO J. **16:**5501–5508.
32. **Schuck, S., and K. Simons.** 2004. Polarized sorting in epithelial cells: raft clustering and the biogenesis of the apical membrane. J. Cell Sci. **117:**5955–5964.
33. **Shikata, K., Y. Suzuki, J. Wada, K. Hirata, M. Matsuda, H. Kawashima, T. Suzuki, M. Iizuka, H. Makino, and M. Miyasaka.** 1999. L-selectin and its ligands mediate infiltration of mononuclear cells into kidney interstitium after ureteric obstruction. J. Pathol. **188:**93–99.
34. **Simons, K., and D. Toomre.** 2000. Lipid rafts and signal transduction. Nat. Mol. Cell Biol. Rev. **1:**31–41.
35. **Stein, C., V. Gieselmann, J. Kreysing, B. Schmidt, R. Pohlmann, A. Waheed, H. E. Meyer, J. S. O'Brien, and K. von Figura.** 1989. Cloning and expression of human arylsulfatase A. J. Biol. Chem. **264:**1252–1259.
36. **Suzuki, T., A. Sometani, Y. Yamazaki, G. Horiike, Y. Mizutani, H. Masuda, M. Yamada, H. Tahara, G. Xu, D. Miyamoto, N. Oku, S. Okada, M. Kiso, A. Hasegawa, T. Ito, Y. Kawaoka, and Y. Suzuki.** 1996. Sulphatide binds to human and animal influenza A viruses, and inhibits the viral infection. Biochem. J. **318:**389–393.
37. **Suzuki, T., A. Portner, R. A. Scroggs, M. Uchikawa, N. Koyama, K. Matsuo, Y. Suzuki, and T. Takimoto.** 2001. Receptor specificities of human respiroviruses. J. Virol. **75:**4604–4613.
38. **Suzuki, T., T. Takahashi, D. Nishinaka, M. Murakami, S. Fujii, K. I. Hidari, D. Miyamoto, Y. T. Li, and Y. Suzuki.** 2003. Inhibition of influenza A virus sialidase activity by sulfatide. FEBS Lett. **553:**355–359.
39. **Suzuki, Y., H. Nishi, K. Hidari, Y. Hirabayashi, M. Matsumoto, T. Kobayashi, S. Watarai, T. Yasuda, J. Nakayama, H. Maeda, T. Katsuyama, M. Kanai, M. Kiso, and A. Hasegawa.** 1991. A new monoclonal antibody directed to sialyl alpha 2-31actoneotetraosylceramide and its application for detection of human gastrointestinal neoplasmas. J. Biochem. **109:**354–360.
40. **Talts, J. F., Z. Andac, W. Gohring, A. Brancaccio, and R. Timpl.** 1999. Binding of the G domains of laminin alpha1 and alpha2 chains and perlecan to heparin, sulfatides, alpha-dystroglycan and several extracellular matrix proteins. EMBO J. **18:**863–870.
41. **Toledo, M. S., E. Suzuki, K. Handa, and S. Hakomori.** 2004. Cell growth regulation through GM3-enriched microdomain (glycosynapse) in human lung embryonal fibroblast WI38 and its oncogenic transformant VA13. J. Biol. Chem. **279:**34655–34664.
42. **Wurzer, W. J., O. Planz, C. Ehrhardt, M. Giner, T. Silberzahn, S. Pleschka, and S. Ludwig.** 2003. Caspase 3 activation is essential for efficient influenza virus propagation. EMBO J. **22:**2717–2728.
43. **Yaghootfam, A., F. Schestag, T. Dierks, and V. Gieselmann.** 2003. Recognition of arylsulfatase A and B by the UDP-*N*-acetylglucosamine: lysosomal enzyme *N*-acetylglucosamine-phosphotransferase. J. Biol. Chem. **278:**32653–32661.
44. **Zhang, J., A. Pekosz, and R. A. Lamb.** 2000. Influenza virus assembly and lipid raft microdomains: a role for the cytoplasmic tails of the spike glycoproteins. J. Virol. **74:**4634–4644.